Inorganic Chemistry

ARTICLE

pubs.acs.org/IC

Photo- and Electrochemical Redox Behavior of Cyclometalated Ru(II) Complexes Having a 3-Phenylbenzo[*b*][1,6]naphthyridine Ligand

Sumanta Kumar Padhi and Koji Tanaka*

Department of Life and Coordination-Complex Molecular Science, Institute for Molecular Science, 5-1, Higashiyama, Myodaiji, Okazaki, Aichi 444-8787, Japan

Supporting Information

ABSTRACT: Cyclometalated Ru(II) complexes having a 3-phenylbenzo[*b*][1,6]naphthyridine (**phbn**) ligand have been synthesized and characterized by spectroscopic methods. The photo- and electrochemical redox behavior of the complexes are demonstrated. Complex [Ru(**phbn**)(bpy)$_2$]PF$_6$ ([**1**]PF$_6$) readily undergoes proton coupled two electron reduction by chemical, electrochemical, and photochemical methods to generate [Ru(**phbnHH**)(bpy)$_2$]PF$_6$ ([**1HH**]PF$_6$). The photochemical oxidation of [**1HH**]PF$_6$ was also observed in presence of *p*-chloranil.

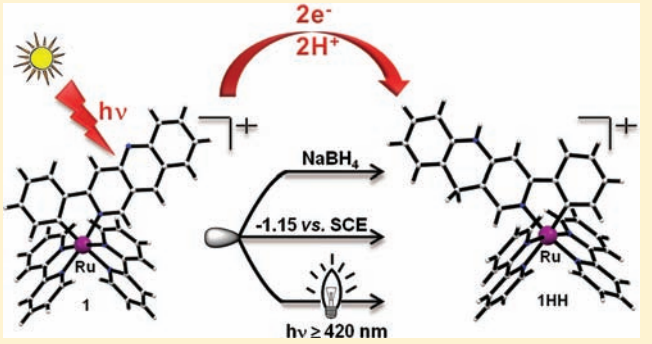

1. INTRODUCTION

At present, the world highly demands renewable energy resources for the storage of solar energy. One of the key interests for environmental scientists is to find out the alternative sources for the utilization of light driven energy in the form of chemical energy.[1] In the realm of coordination chemistry ruthenium-poly pyridyl complexes have been paid superior attention for molecular light-to-chemical energy conversion because of their unique photophysical properties and chemical stabilities.[2] The photoinduced proton coupled "multielectronic reservoirs" of ruthenium complexes are far less common.[3] The Brewer,[4] MacDonnell,[5] Nocera,[6] and Rau[7] groups have reported the storage of more than one photoexcited electron into the π^* orbital of the poly pyridyl ligands in the presence of sacrificial electron donors upon irradiation with visible light. Very recently our group has developed two, four, and six reversible electron storing ability of [Ru(bpy)$_2$(**pbn**)](PF$_6$)$_2$, [Ru(bpy)(**pbn**)$_2$](PF$_6$)$_2$, and [Ru(**pbn**)$_3$](PF$_6$)$_2$ (**pbn** = 2-(2-pyridyl)benzo[*b*]-1,5-naphthyridine), respectively.[8] However, there are no reports of the photochemical redox behavior of a cyclometalated complex. Recently we have reported the two electron reduction of the cyclometalated complex [Ru(**pad**)(bpy)$_2$]PF$_6$ to [Ru(**padHH**)(bpy)$_2$]PF$_6$ under controlled potential electrolysis at −1.5 V vs SCE (**pad** = 2-(pyridin-2-yl)acridine; **padHH** = 2-(pyridin-2-yl)-9,10-dihydroacridine).[9] In this Article we report the synthesis, characterization, and the proton coupled two electron reduction of [Ru(**phbn**)(bpy)$_2$]PF$_6$ ([**1**]PF$_6$; **phbn** = 3-phenylbenzo-[*b*][1,6]naphthyridine).

Scheme 1. Synthesis of Ligand phbn

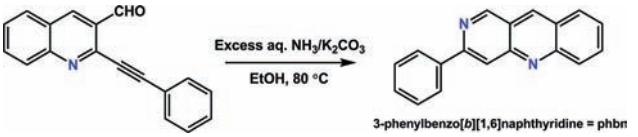

2. RESULTS AND DISCUSSION

2.1. Syntheses. The ligand 3-phenylbenzo[*b*][1,6]naphthyridine (**phbn**) was synthesized according to the synthetic procedure outlined in Scheme 1. A reaction mixture of 2-(2-phenylethynyl)quinoline-3-carbaldehyde and K_2CO_3 in ethanol upon condensation with an excess aqueous NH_3 solution at 80 °C affords an yellowish microcrystalline product of 3-phenylbenzo[*b*][1,6]naphthyridine (**phbn**) (Yield: 47%). Treatment of **phbn** with [(η^6-C_6H_6)$RuCl_2$]$_2$, $NaPF_6$, and NaOH in acetonitrile provides [Ru(**phbn**)(CH_3CN)$_4$]PF$_6$ (Yield: 97%). Further addition of 2 equiv of 2,2′-bypiridyl with [Ru(**phbn**)(CH_3CN)$_4$]-PF$_6$ in 2-methoxyethanol gives [Ru(**phbn**)(bpy)$_2$]PF$_6$ ([**1**]PF$_6$) (Yield: 72%) (Scheme 2).

The complex [**1**]PF$_6$ was reduced to [Ru(**phbnHH**)-(bpy)$_2$]PF$_6$ ([**1HH**]PF$_6$) by chemical, electrochemical, and photochemical methods (Scheme 3). By the treatment of [**1**]PF$_6$ with $NaBH_4$ in methanol/H_2O mixture (9:1 v/v) under nitrogen atmosphere, [**1HH**]PF$_6$ was isolated in a very good yield of 80%. The purple color of [**1**]PF$_6$ gradually turned to brownish red under the controlled potential electrolysis at −1.15 V

Received: June 6, 2011
Published: September 28, 2011

dx.doi.org/10.1021/ic201207x | *Inorg. Chem.* 2011, 50, 10718–10723

Scheme 2. Synthesis of $[Ru(phbn)(bpy)_2]PF_6$ ($[1]PF_6$)

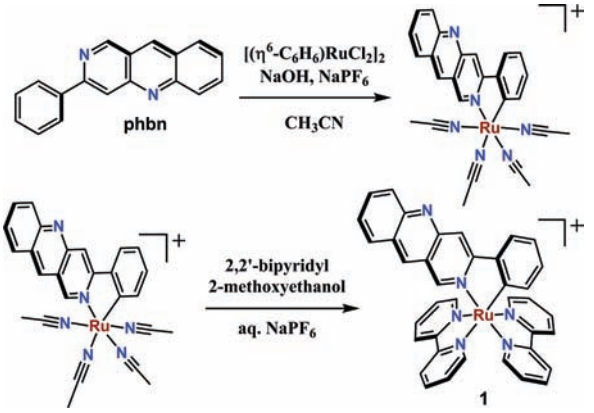

Scheme 3. Synthesis of ($[1HH]PF_6$)

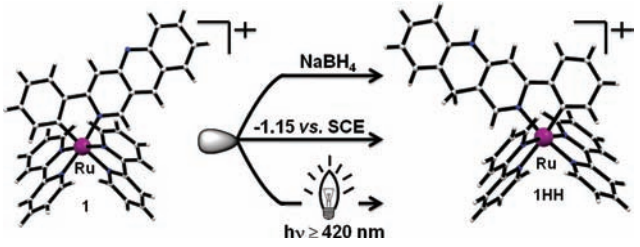

(vs SCE) in CH_3CN/H_2O (9:1 v/v) containing Bu_4NPF_6 as a supporting electrolyte (0.1 M), and $[1HH]PF_6$ was produced after consumption of 2 equiv of electrons in the electrolysis (Yield 55%). The high-resolution electrospray ionization (HR-ESI) mass spectra, cyclic voltammogram, and the UV−vis spectra of the resultant product are consistent with those of $[1HH]PF_6$ obtained by the chemical reduction method. The ^1H NMR spectrum of $[1HH]PF_6$ in CD_3OD displayed 17 different signals with a total intensity of 29 protons, out of which 27 are in the aromatic region generated from two bpy and a **phbnHH** ligand. An AB patterned doublet was observed at 3.36 {1H, d, (J, H_z) = 19.53}, 3.52 {1H, d, (J, H_z) = 18.93} ppm because of the germinal coupling of the methylene protons.

2.2. Molecular Structure. In complex $[1]PF_6 \cdot CH_3COCH_3$, the asymmetric unit consists of a *mono*-cationic part $[1]^+$, a PF_6^- counteranion, and an acetone as solvent of crystallization. Two 2,2′-bipyridyl and one NC coordinating **phbn** generate a *pseudo*-octahedral geometry at the metal center. A perspective view of $[1]^+$ is displayed in Figure 1a. Here Ru−N bond distances are much longer than the σ-Ru1−C1 2.004(7) Å. A longer Ru1−N4 2.120(6) Å is due to the *trans*-influence of the σ-coordinated sp^2-C1 atom. The torsional angle 4.6(1)° between the two planes due to the benzonapthyridine moiety and the phenyl plane is less than that of the $[Ru(\mathbf{phbn})(CH_3CN)_4]PF_6$ complex (see Supporting Information, Figure S5). The unit cell of $[1HH]PF_6 \cdot CH_3OH$ consists of a *mono*-cationic part $[1HH]^+$, a PF_6^- counteranion, and a methanol as solvent of crystallization. The molecular representation of $[1HH]^+$ has been displayed in Figure 1b. Because of the *trans*-influence of σ-coordinated sp^2-C1 atom, the Ru1−N4 2.102(2) Å is longer than the Ru1−C1 2.032(4) Å bond distance. The torsional angle 2.1(1)° between the two planes due to the 5,10-dihydro-benzo[*b*][1,6]naphthyridine moiety and the phenyl plane is less than that of the $[Ru(\mathbf{phbn})(CH_3CN)_4]PF_6$ as well as that of the $[1]PF_6$ complex. Crystal data and refinement parameters are tabulated in Table 1. The most important thing to notice between $[1]^+$ and $[1HH]^+$ is the carbon center C17,which is respectively sp^2 and sp^3 hybridized in these complexes. The bond lengths of C10−C17 [1.377(11) and 1.426(7) Å] and C12−C17 [1.395-(11) and 1.550(8) Å] significantly vary from the oxidized to the reduced complex.

2.3. Optical Properties. In the visible region 400−600 nm each of these complexes exhibits the metal-to-ligand charge-transfer (MLCT) band. The intraligand charge transfer (ILCT) peaks that appeared in the UV region of 250−280 nm are of $n \rightarrow \pi^*$ (from **phbn** and **phbnHH**) origin (Figure 2 a, b, and c). The $\pi \rightarrow \pi^*$ transitions occur in the 285−375 nm region. Under protic conditions the UV−vis spectra of $[1]PF_6$ shows a bathochromic shift in the MLCT absorption band from 535 to 740 nm based on the **phbn** ligand as the color changes from purple to orange. It causes the decrease of energy of the π^* orbital in **phbn** after protonation, resulting in a red shift for the $Ru(t_{2g}) \rightarrow \mathbf{phbn}(\pi^*)$ orbital. The pK_a of $[1H]^{2+}$ was determined to be 3.65 from the pH dependent UV−vis spectra in (CH_3CN/H_2O (1:9, v/v) solution (Supporting Information, Figure S6). The complex $[1]PF_6$ exhibits emission maximum at 860 nm, and $[1HH]PF_6$ emits at 865 nm upon excitation at 550 nm (Table 2 and Supporting Information, Figure S7).

2.4. Photochemical Reduction and Oxidation. The continuous photolysis at ($\lambda \geq 420$ nm) of a 0.1 mM solution of $[1]PF_6$ in CH_3CN/Et_3N or CH_3CN/triethanolamine (CH_3CN/TEOA) (4:1, v/v) causes a decrease in the absorption bands of $[1]^+$ (λ_{max} = 550 nm) and the appearance of a new species with bands (λ_{max} = 425 nm) as shown in Figure 3 with a gradual change in color of $[1]PF_6$ from purple to brownish red (Table 3). The HR-ESI mass spectrum of the final solution displayed a parent peak at m/z 671.15 found 671.18 (calculated with z = 1), consistent with the formation of $[1HH]^+$ by the reaction of two protons and two photo-produced electrons (yield 57%). In our previous findings of photochemical reduction of $[Ru(bpy)_2(\mathbf{pbn})]^{2+}$, photochemically generated $[Ru(bpy)_2(\mathbf{pbn}^{-\bullet})]^+$ undergoes protonation, and the resultant $[Ru(bpy)_2(\mathbf{pbnH}^{\bullet})]^{2+}$ forms an intermediate $\pi \cdots \pi$ dimer $\{[Ru(bpy)_2(\mathbf{pbnH}^{\bullet})]^{2+}\}_2$. The subsequent proton coupled electron transfer between the two $[Ru(bpy)_2(\mathbf{pbnH}^{\bullet})]^{2+}$ moieties in the dimer causes the disproportionation reaction to produce $[Ru(bpy)_2$-$(\mathbf{pbnHH})]^{2+}$ and $[Ru(bpy)_2(\mathbf{pbn})]^{2+}$. In the present study, we could not observe any intermediate species in the absorption spectra during the photo irradiation. It is expected that the one electron reduced species might be an unstable species. Here we propose that (Scheme 4) the radical ligand may generate upon the initial reduction, protonates (Step 1), and then disproportionates ($K_{dis} = 3.0 \times 10^{-14}$; K_{dis} is the disproportionation constant) through electron and proton transfer to afford $[1HH]^+$ and $[1]^+$ (Step 2). The similar proton-coupled two electron reduction of $[1]^+$ to $[1HH]^+$ was also observed in (acetone/TEOA) solution (4:1, v/v) (Table 3). The (0−0) transition energy of $[1]^+$ in CH_3CN at 298 K is calculated to be 1.44 eV based on the emission maximum 860 nm. The excited state redox potential for the (Ru^{II*}/Ru^{I}) couple is correlated with $E_{1/2}$ ($\mathbf{pbn}^{-\bullet}/\mathbf{pbn}$) and $E_{em}(0-0)$, eq 1,[8a,11a] and determined to be 0.83 V vs SCE. The redox potential of the (Ru^{II*}/Ru^{I}) couple is located at more positive potential than the oxidation potential of sacrificial agents therefore indicates that electron transfer

dx.doi.org/10.1021/ic201207x |*Inorg. Chem.* 2011, 50, 10718–10723

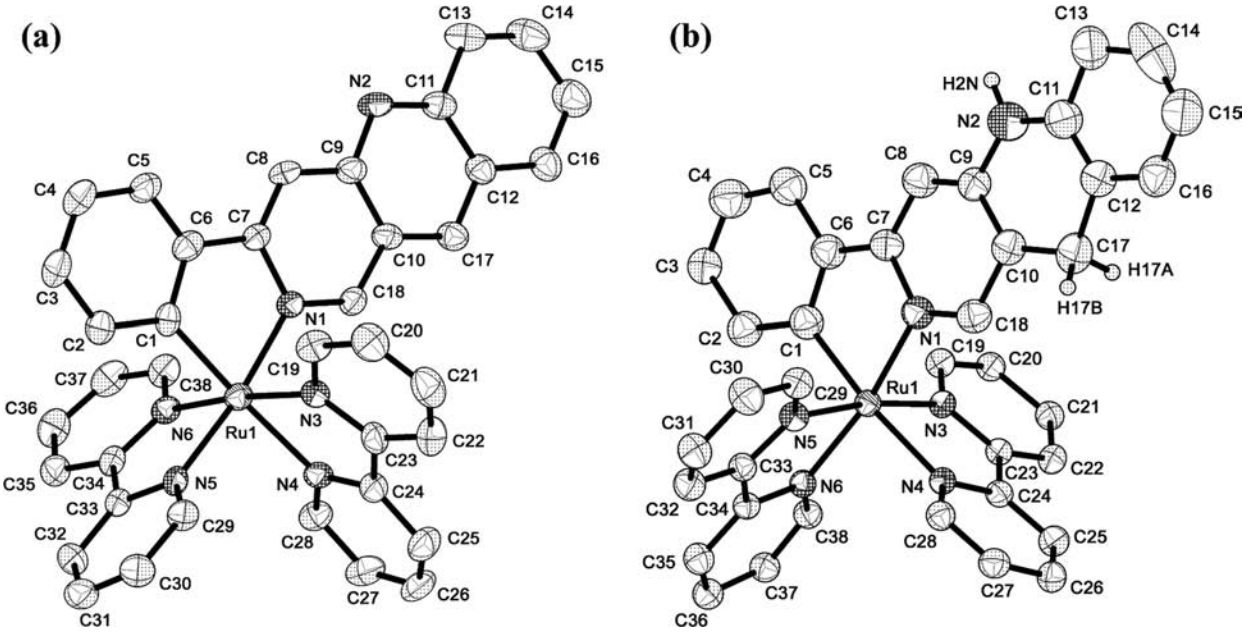

Figure 1. ORTEP (30% probability) of (a) $[\mathbf{1}]^+$ and (b) $[\mathbf{1HH}]^+$.

Table 1. Crystal Data and Refinement Parameters

	$[\mathbf{1}]PF_6 \cdot CH_3COCH_3$	$[\mathbf{1HH}]PF_6 \cdot CH_3OH$
CCDC number	809691	809692
empirical formula	$C_{41}H_{33}F_6N_6OPRu$	$C_{39}H_{33}F_6N_6OPRu$
formula weight	812.04	847.75
temperature (K)	153(2)	295(2)
wavelength, Å	0.71073	0.71073
crystal system	monoclinic	monoclinic
space group	$P2_1/c$	$P2_1/c$
a, Å	12.310(6)	10.327(3)
b, Å	27.225(12)	21.854(5)
c, Å	12.262(6)	15.447(4)
α, deg	90	90
β, deg	117.337(6)	96.185(3)
γ, deg	90	90
V, Å^3	3651(3)	3465.9(16)
Z	4	4
D_{calc} (g cm^{-3})	1.586	1.625
μ, (mm^{-1})	0.548	0.575
[a]GOF on F^2	0.999	1.018
R $[I > 2\sigma(I)]$	[b]R_1 = 0.0678, [c]wR_2 = 0.1911	[b]R_1 = 0.0430, [c]wR_2 = 0.1370
R indices (all data)	[b]R_1 = 0.0833, [c]wR_2 = 0.2201	[b]R_1 = 0.0469, [c]wR_2 = 0.1406

[a] GOF = $[\Sigma w(F_o^2 - F_c^2)^2/(M-N)]^{1/2}$ (M = number of reflections, N = number of parameters refined). [b] $R_1 = \Sigma||F_o| - |F_c||/\Sigma|F_o|$. [c] $wR_2 = [\Sigma w(F_o^2 - F_c^2)^2/\Sigma w(F_o^2)]$.

from TEA or TEOA to the ruthenium center is highly possible.

$$E(Ru^{II}*/Ru^{I}) = E_{1/2}(\mathbf{phbn}^{-\bullet}/\mathbf{phbn}) + E_{em}(0-0) \quad (1)$$

The photochemical reduction of $[\mathbf{1}]^+$ in CH_3CN/Et_3N solution (4:1, v/v) becomes faster in the presence of 1 equiv of

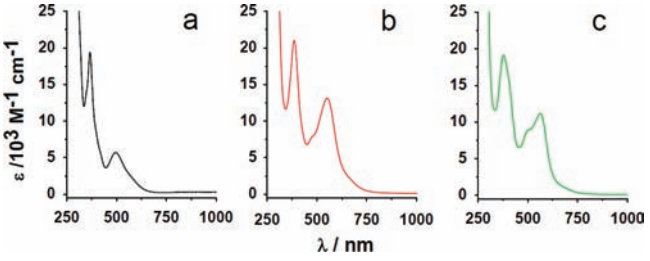

Figure 2. UV−vis Spectra of (a) $[Ru(\mathbf{phbn})(CH_3CN)_4]PF_6$, (b) $[\mathbf{1}]PF_6$, and (c) $[\mathbf{1HH}]PF_6$ in 0.1 × 10^{-3} M CH_3CN.

Table 2. Luminescence Data[a]

complexes	λ_{ex} (nm)	λ_{em} (nm)	λ_{abs} (nm)(ε [×10^4 M^{-1} cm^{-1}])	Φ	reference
$[Ru(\mathbf{bpy})_3](PF_6)_2$	460	615	451(1.4)	0.062	10
$[Ru(\mathbf{bpy})_2(ppy)](PF_6)_2$	545	800	546(1.0)		10
$[Ru(\mathbf{phbn})(bpy)_2]PF_6$	550	860	550(1.3)	0.005	this work
$[Ru(\mathbf{phbnHH})(bpy)_2]PF_6$	550	865	565(1.1)	0.006	this work
$[Ru(\mathbf{pad})(bpy)_2]PF_6$	535	750	530(0.78)	0.003	this work

[a] The emission spectra were recorded in CH_3CN at room temperature.

hydroquinone. The reduction process does not proceed only in presence of hydroquinone without the sacrificial agent Et_3N. It is expected that the process is accelerated here because of the proton source of hydroquinone. However under similar condition the presence of NAD$^+$/NADH model ligand 2-(pyridin-2-yl)-9,10-dihydroacridine (**padHH**) retards the photoreduction process. This is due to the role of Et_3N which usually accelerates deprotonation of **padHH** rather immediate involvement as sacrificial agent (Scheme S4).[11b−d]

The photochemical oxidation of $[\mathbf{1HH}]^+$ to $[\mathbf{1}]^+$ was also observed in the presence of 1 equiv of *p*-chloranil. The final product was isolated and confirmed from the HR-ESI mass

dx.doi.org/10.1021/ic201207x |*Inorg. Chem.* 2011, 50, 10718–10723

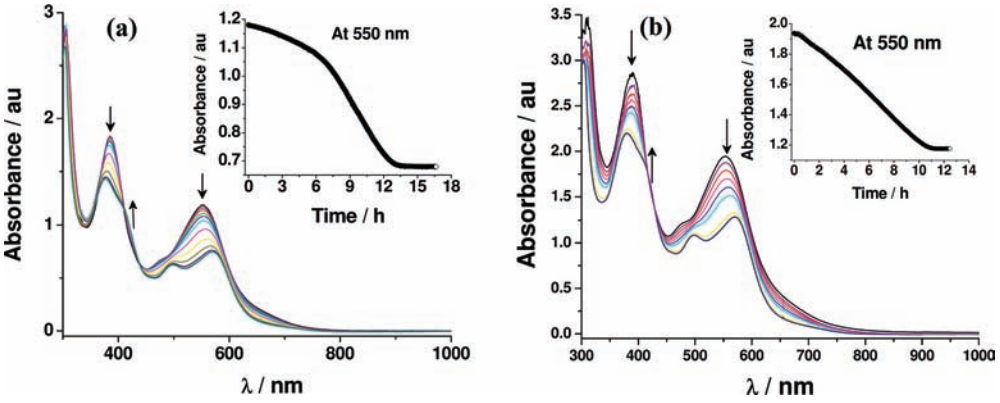

Figure 3. Change in UV−vis spectra of photoinduced reduction of $[\mathbf{1}]PF_6$ in 0.1×10^{-3} M (a) CH_3CN/TEA 4:1 v/v, (b) CH_3CN/TEOA 4:1 v/v upon irradiation with $h\nu \geq 420$ nm; inset is the absorbance vs time profile at 550 nm.

Table 3. Reaction Conditions for the Photochemical Reduction of $[\mathbf{1}]PF_6$

sacrificial agent	solvent[a]	additive	time/h	[b] $k_{relative}$/s
TEA	CH_3CN:TEA (4:1 v/v)	none	13.0	-2.38×10^{-5}
TEOA	CH_3CN:TEOA (4:1 v/v)	none	11.0	-5.33×10^{-6}
TEOA	CH_3COCH_3:TEOA (4:1 v/v)	none	7.0	-3.70×10^{-7}
TEA	CH_3CN:TEA (4:1 v/v)	hydroquinone	8.75	-6.27×10^{-5}
TEA	CH_3CN:TEA (4:1 v/v)	padHH	14.5	-2.57×10^{-5}

[a] The concentration of the solution was 0.1×10^{-3} M and irradiated with $h\nu \geq 420$ nm. [b] $k_{relative}$ is the 1st order rate constant for the photochemical reduction of $[\mathbf{1}]PF_6$.

spectra as well as proton NMR spectra (Yield 78%). The isolation of two electron oxidized product $[\mathbf{1}]^+$ occurs with release of hydride to *p*-chloranil. However the reaction does not proceed under bare conditions upon irradiation. In this case the peak at 550 nm increases with a decrease in the intensity of the band at 450 nm which is similar to the UV−vis spectra of $[\mathbf{1}]^+$ after the completion of the reaction. The redox potential of the (Ru^{II*}/Ru^{I}) couple is much less compared to the oxidation potential of **phbnHH** in $[\mathbf{1HH}]^+$ and consequently electron transfer from **phbnHH** to the ruthenium center is not possible. Therefore, the *p*-chloranil was chosen here as the oxidizing agent. Very recently we have reported the cyclometalated complex [Ru(**pad**)-$(bpy)_2]PF_6$ which does not undergo the photochemical reduction under similar conditions.[9]

2.5. Cyclic Voltammetry. The cyclic voltammogram of $[\mathbf{1}]$-PF_6 in dry CH_3CN exhibits the reversible (Ru^{II}/Ru^{III}) redox couple at $E_{1/2}$ = +0.51 V(vs SCE). One reversible cathodic wave at −0.92 V was observed due to (**phbn**/**phbn**$^{-\bullet}$) along with two reversible (bpy, bpy/bpy$^{-\bullet}$, bpy) and (bpy$^{-\bullet}$, bpy/bpy$^{-\bullet}$, bpy$^{-\bullet}$) redox couples at $E_{1/2}$ = −1.72 V and −2.02 V, respectively (Supporting Information, Figure S8). On addition of 2 equiv of acetic acid to the solution the cathodic peak at −0.92 V underwent an anodic shift to −0.84 V. Consumption of 2F/mol of electrons in the exhaustive controlled potential electrolysis of 1 mM $[\mathbf{1}]PF_6$ solution in CH_3CN/H_2O (9:1 v/v) containing Bu_4NPF_6 as a supporting electrolyte (0.1 M) at −1.15 V (vs SCE) clarified the irreversible redox reaction as proton coupled two-electron reduction of **phbn** affording **phbnHH**. In case of $[\mathbf{1HH}]PF_6$ the two redox couples at −1.67 and −1.92 V are respectively due to the reduction of (bpy, bpy/bpy$^{-\bullet}$, bpy) and (bpy$^{-\bullet}$, bpy/bpy$^{-\bullet}$, bpy$^{-\bullet}$) (Supporting Information, Figure S9). An irreversible oxidation wave was observed at the anodic end at +1.15 V and assigned to **phbnHH** based oxidation along with the reversible redox couples for (Ru^{II}/Ru^{III}) at +0.35 V and a shoulder at +0.55 V assigned to (Ru^{III}/Ru^{IV}). Over the pH range ≥3.5, the slope of the redox potential of (Ru^{II}**phbn**/Ru^{II}**phbnHH**) is −59 mV/pH in CH_3CN/H_2O (1:1 v/v) containing 0.1 M phosphate buffer.

2.6. Electrochemical Reduction and Electronic Absorption. The electrolytic reduction 1.0 mM of $[\mathbf{1}]PF_6$ containing Bu_4NPF_6 as a supporting electrolyte (0.1 M) in acetonitrile/H_2O (9:1 v/v) mixture under controlled potential electrolysis was carried out at −1.15 V vs SCE under argon atmosphere at 25 °C. An electrolysis UV-cell of path length 0.05 cm which consists of three components: the working (platinum mesh) and the counter (platinum wire) electrodes was used. The reference electrode ($Ag/AgNO_3$, +0.30 V vs SCE) was separated from the working compartment by a Vycor glass. In this case the peak at 550 nm decreases with an increase in the intensity of the band at 450 nm which is similar to the UV−vis spectra of $[\mathbf{1HH}]^+$ after the completion of the reaction (Figure 4). The final product was isolated and confirmed from the HR-ESI mass spectra as well as proton NMR spectra.

3. EXPERIMENTAL SECTION

3.1. Instrumentation and Materials. All the manipulations were carried out using standard Schlenk techniques under nitrogen atmosphere. Solvents like dimethylformamide (DMF), diethylether, dichloromethane, acetonitrile, methanol, ethanol, 2-methoxyethanol, and hexane were dried, degassed, and stored under nitrogen atmosphere prior to use. NMR spectra were recorded on a JEOL JNM-A500 spectrometer (500 MHz for ^{1}H) at room temperature. High resolution ESI mass spectra were recorded on a Waters Micromass LCT. The UV−vis−NIR spectra were recorded on a Shimadzu UVPC-3100 PC

dx.doi.org/10.1021/ic201207x |*Inorg. Chem.* 2011, 50, 10718–10723

UV−vis−NIR scanning spectrophotometer or on an Agilent 8543A diode-array spectrophotometer. Emission spectra were recorded on a JASCO FP-6600 spectrofluorometer. Both cyclic voltammetry and controlled-potential electrolysis were carried out under argon atmosphere. Cyclic voltammetry was carried out using an ALS/Chi model 660A electrochemical analyzer under argon atmosphere at 25 °C at a scan rate of 50 mV in acetonitrile containing Bu_4NPF_6 as a supporting electrolyte (0.1 M) with a complex concentration of 1.0 mM. The working, auxiliary, and reference electrodes were AS Glassy Carbon electrode, platinum wire, and $Ag/AgNO_3$ (0.01 M, BAS RE-5, +0.30 V vs SCE), respectively.

X-ray Crystallographic Analysis. X-ray data were collected at 100 K (for $[Ru(\mathbf{phbn})(CH_3CN)_4]PF_6$), at 153 K for $[\mathbf{1}]PF_6 \cdot CH_3COCH_3$, and at 295 K for $[\mathbf{1HH}]PF_6 \cdot CH_3OH$ on a Rigaku Saturn CCD area detector with graphite monochromatic Mo−Kα radiation (λ = 0.71070 Å) and processed using Crystal Clear.[12a] The structure was solved by direct method (SHELX-97) and expanded using Fourier techniques. Non-hydrogen atoms located from the difference Fourier maps were refined anisotropically by full-matrix least-squares on F^2 using SHELXL-97.[12b] All hydrogen atoms included at the calculated positions were refined isotropically using a riding model. The CCDC numbers of the complexes are 809690−809692.

Scheme 4. Mechanistic Approach for the Photochemical Reduction of $[\mathbf{1}]PF_6$

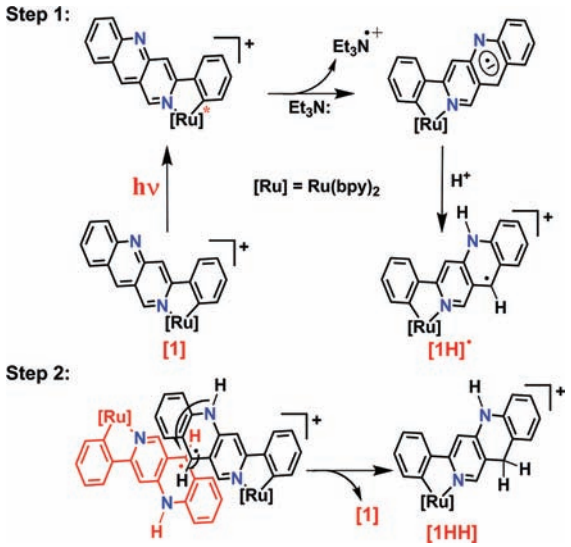

Photochemical Reduction and Oxidation. Photochemical reduction of $[\mathbf{1}]^+$ were conducted in nitrogen-bubbled 0.1 mM CH_3CN/TEA (4: 1, v/v) or CH_3CN/TEOA (4: 1, v/v) solution at 293 K and for the oxidation of 0.1 mM CH_3CN solution of $[\mathbf{1HH}]^+$ containing 1 equiv of *p*-chloranil was irradiated with light through a cutoff filter (TOSHIBA L-42) using a 150 W xenon lamp.

Electrochemical Reduction. The electrolytic reduction of $[\mathbf{1}]PF_6$ was carried out in acetonitrile/H_2O (9:1 v/v) mixture containing Bu_4NPF_6 as a supporting electrolyte (0.1 M) with a complex concentration of 1.0 mM under controlled potential electrolysis at −1.15 V vs SCE under argon atmosphere at 25 °C. An electrolysis cell which consists of three components: the working (glassy carbon) and the counter (platinum plate) electrodes were separated by an anion-exchange membrane; Nafion 117 was used. The reference electrode ($Ag/AgNO_3$, +0.30 V vs SCE) was separated from the working compartment by a Vycor glass.

3.2. General Procedures. The materials like 2-chloro-3-quinoline carboxaldehyde[13a] and 2-(2-phenylethynyl)quinoline-3-carbaldehyde[13b] were synthesized according to the literature procedures. The ligand 3-phenylbenzo[*b*][1,6]naphthyridine (**phbn**)[13c] was prepared using the synthetic procedure outlined in Scheme 1. The details of synthesis are provided in the Supporting Information. The complex syntheses are mentioned in Scheme 2.

*3.2.1. Synthesis of [Ru(**phbn**)(CH$_3$CN)$_4$]PF$_6$.* A suspension of $[(\eta^6\text{-}C_6H_6)RuCl_2]_2$ (0.256 g, 0.5 mmol), **phbn** (0.256 g, 1 mmol), NaOH (0.04 g, 1 mmol), and $NaPF_6$ (0.336 g, 2 mmol) in 60 mL of CH_3CN was stirred for 48 h at 60 °C. The crude mixture was purified by column chromatography on neutral alumina using CH_2Cl_2/EtOH and isolated as the pure product (0.650 g, 1.15 mmol, yield: 97%). The red colored block like crystals of $[Ru(\mathbf{phbn})(CH_3CN)_4]PF_6$ suitable for X-ray crystallography were grown from the slow evaporation of acetonitrile solution. HRMS (ESI): Calc. for $C_{26}H_{23}N_6Ru$ $[Ru(\mathbf{phbn})(CH_3CN)_4]^+$ *m/z* 521.10 found 521.19 and $C_{24}H_{20}N_5Ru$ $[Ru(\mathbf{phbn})(CH_3CN)_3]^+$ *m/z* 480.08 found 480.15. Calc. for $C_{26}H_{23}F_6N_6PRu$: %C 46.92, %H 3.48, %N 12.63; found %C 47.03, %H 3.51, %N 12.56. The ^{1}H NMR (500 MHz, CD_3CN): δ, ppm (*J*, Hz): 1.95 (3H, s), 2.01(6H, s), 2.55 (3H, s), 6.99(1H, t, 7), 7.10 (1H, t, 7), 7.64 (1H, t, 7.63), 7.96 (3H, m), 8.16 (2H, t, 11.6), 8.34 (1H, s), 9.15 (1H, s), 10.00(1H, s).

*3.2.2. Synthesis of ([**1**]PF$_6$).* To a solution of (0.400 g, 0.60 mmol) of $[Ru(\mathbf{phbn})(CH_3CN)_4]PF_6$ in 50 mL of 2-methoxyethanol was added with (0.190 g, 1.2 mmol) of 2,2′-bipyridyl and saturated aqueous solution of $NaPF_6$ (0.100 g, 0.6 mmol). The above reaction mixture

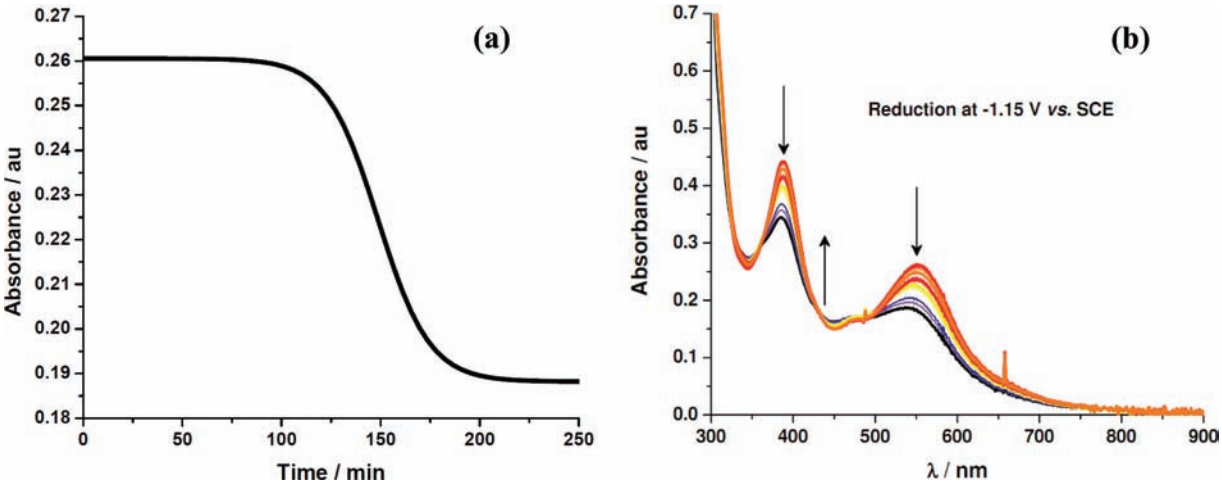

Figure 4. Electrochemical reduction of $[\mathbf{1}]PF_6$ in CH_3CN:H_2O (9:1) containing Bu_4NPF_6 as a supporting electrolyte (0.1 M) with a complex concentration of 1.0 mM. (a) Absorbance vs time profile at 550 nm during controlled potential electrolysis. (b) The change in UV−vis spectra.

dx.doi.org/10.1021/ic201207x |*Inorg. Chem.* 2011, 50, 10718–10723

was refluxed at 80 °C for 24 h. The crude product contains a mixture which was evaporated to dryness and purified by column chromatography on neutral alumina using CH_2Cl_2/EtOH by 99:1 (v/v) ratio to give $[\mathbf{1}]PF_6$ of (0.350 g, 0.43 mmol, Yield: 72%). Block like dark crystals suitable for X-ray analysis were isolated from the slow evaporation of acetone solution of $[\mathbf{1}]PF_6$. HRMS (ESI): Calc. for $C_{38}H_{27}N_6Ru$ $[\mathbf{1}]^+$ *m/z* 669.13 found 669.50. Calc. for $C_{38}H_{27}F_6N_6PRu$: %C 56.09, %H 3.34, %N 10.33; found %C 56.20, %H 3.71, %N 10.11. The ^{1}H NMR (500 MHz, CD_3OD): δ, ppm (*J*, Hz): 6.15 (1H, d, 7.35), 6.55(1H, t, 12.33), 6.69 (1H, t, 7.95), 6.91−7.03 (3H, m), 7.21−7.32 (3H, m), 7.50 (1H, d, 5.5), 7.53−7.58 (2H, m), 7.61−7.66 (1H, m), 7.67−7.73 (3H, m), 7.77 (1H, d, 8.55), 7.81−7.85 (2H, m), 8.01 (1H, d, 5.45), 8.18(1H,s), 8.19−8.29(3H, m), 8.38−8.43(1H, m), 8.48(1H, s), 8.58 (1H, s).

*3.2.3. Synthesis of ([**1HH**]PF_6).* A solution of $[\mathbf{1}]PF_6$ (0.100 g, 0.12 mmol) in a two-necked round-bottom flask containing 20 mL of methanol/H_2O (9:1 v/v) was purged under nitrogen for 30 min at −10 °C. The solid $NaBH_4$ (10 mg, 0.26 mmol) was directly added into the solution allowed to stir for 3 h. A brownish red colored precipitate was collected under centrifugation followed by washing with ice-cold methanol/H_2O (9:1 v/v) mixture to give pure $[\mathbf{1HH}]PF_6$ (0.08 g (0.100 mmol) Yield: 80%). Block like dark red color crystals suitable for X-ray analysis were isolated from the slow evaporation of methanolic solution of $[\mathbf{1HH}]PF_6$. HRMS (ESI): Calc. for $C_{38}H_{29}N_6Ru$ $[\mathbf{1HH}]^+$ *m/z* 671.15 found 671.18. Calc. for $C_{38}H_{29}F_6N_6PRu$: %C 55.95, %H 3.58, %N 10.30; found %C 55.74, %H 3.66, %N 10.14. The ^{1}H NMR (500 MHz, CD_3OD): δ, ppm (*J*, Hz): 3.36 (1H, d, 19.53), 3.52 (1H, d, 18.93), 6.08 (1H,d, 6.75), 6.48−6.58 (4H, m), 6.70(1H, d, 6.7), 6.72(1H, s), 6.78 (1H, t, 7.62), 6.93−6.99 (4H, m), 7.04 (1H, s), 7.19 (1H, t, 6.4), 7.41−7.55 (5H, m), 7.60 (1H, d, 4.9), 7.71−7.76 (2H, m), 7.92 (1H, d, 4.9), 8.13(2H, t, 8.85), 8.24 (1H, d, 7.9), 8.33(1H, d, 8.55).

4. CONCLUSION

The continuous photoirradiation of ($[\mathbf{1}]PF_6$) in CH_3CN/Et_3N or CH_3CN/triethanolamine (CH_3CN/TEOA) (4:1, v/v) under visible light ($\lambda \geq 420$ nm) readily causes the proton coupled two electron reduction with the generation of ($[\mathbf{1HH}]PF_6$). The reduced complex ($[\mathbf{1HH}]PF_6$) was also obtained by chemical as well as electrochemical methods. Photo-oxidation of $[\mathbf{1HH}]^+$ containing 1 equiv of *p*-chloranil in CH_3CN gives the two electron oxidized product $[\mathbf{1}]^+$. The complex $[\mathbf{1HH}]^+$ is an example of two electron reservoir and opens the path to study the utilization of this multielectronic reservoir in various aspects. The photochemical reduction of $[\mathbf{1}]^+$ is expected to proceed through (i) initial radical formation, (ii) protonation, and (iii) disproportionation paths to generate $[\mathbf{1HH}]^+$. A detailed study of the mechanistic path is underway and will be published later.

■ ASSOCIATED CONTENT

Supporting Information. Experimental details (PDF) and crystallographic data files (cif). This material is available free of charge via the Internet at http://pubs.acs.org.

■ AUTHOR INFORMATION

Corresponding Author
*E-mail: ktanaka@ims.ac.jp.

■ ACKNOWLEDGMENT

This work is supported by a Grand-in-Aid for Specially Promoted Research (Grant 20002005) from the Ministry of Education, Culture, Sports, Science, and Technology of Japan.

■ REFERENCES

(1) (a) Grätzel, M.; Moser, J.-E. In *Electron Transfer in Chemistry*; Balzani, V., Ed.; Wiley-VCH: Weinheim, Germany, 2001; Vol. 5, p 589. (b) Goldemberg, J. The promise of clean energy *Energy Policy* **2006**, *34*, 2185–2190.

(2) (a) Balzani, V.; Ceroni, P.; Maestri, M.; Saudan, C.; Vicinelli, V. *Top. Curr. Chem.* **2003**, *228*, 159–191. (b) Balzani, V.; Campagna, S.; Denti, G.; Juris, A.; Serroni, S.; Venturi, M. *Acc. Chem. Res.* **1998**, *31*, 26–34. (c) Hagfeldt, A.; Grätzel, M. *Acc. Chem. Res.* **2000**, *33*, 269–277. (d) Brown, G. M.; Brunschwig, B. S.; Creutz, C.; Endicott, J. F.; Sutin, N. *J. Am. Chem. Soc.* **1979**, *101*, 1298–1300.

(3) (a) Ali, M. M.; Sato, H.; Haga, M.-a.; Tanaka, K.; Yoshimura, A.; Ohno, T. *Inorg. Chem.* **1998**, *37*, 6176–6180. (b) Ghaddar, T. H.; Wishart, J. F.; Thompson, D. W.; Whitesell, J. K.; Fox, M. A. *J. Am. Chem. Soc.* **2002**, *124*, 8285–8289. (c) Chang, C. C.; Pfennig, B.; Bocarsly, A. B. *Coord. Chem. Rev.* **2000**, *208*, 33–45. (d) Eisner, U.; Kuthan, J. *Chem. Rev.* **1972**, *72*, 1–42. (e) Walsh, C. *Acc. Chem. Res.* **1980**, *13*, 148–165. (f) Stout, D. M.; Meyers, A. I. *Chem. Rev.* **1982**, *82*, 223–243. (g) Ozawa, H.; Haga, M.-a.; Sakai, K. *J. Am. Chem. Soc.* **2006**, *128*, 4926–4927.

(4) (a) Molnar, S. M.; Nallas, G.; Bridgewater, J. S.; Brewer, K. J. *J. Am. Chem. Soc.* **1994**, *116*, 5206–5210. (b) Elvington, M.; Brewer, K. J. *Inorg. Chem.* **2006**, *45*, 5242. (c) Elvington, M.; Brown, J.; Arachchige, S. M.; Brewer, K. J. *J. Am. Chem. Soc.* **2007**, *129*, 10644–10645.

(5) (a) Konduri, R.; Ye, H.; MacDonnell, F. M.; Serroni, S.; Campagna, S.; Rajeshwar, K. *Angew. Chem., Int. Ed.* **2002**, *41*, 3185–3187. (b) Tacconi, N. R.; Lezna, R. O.; Konduri, R.; Ongeri, F.; Rajeshwar, K.; MacDonnell, F. M. *Chem.—Eur. J.* **2005**, *11*, 4327–4339.

(6) (a) Heyduk, A. F.; Nocera, D. G. *Science* **2001**, *293*, 1639–1641. (b) Gray, T. G.; Nocera, D. G. *Chem. Commun.* **2005**, 1540–1542. (c) Esswein, A. J.; Veige, A. S.; Nocera, D. G. *J. Am. Chem. Soc.* **2005**, *127*, 16641–16651.

(7) Rau, S.; Schäfer, B.; Gleich, D.; Anders, E.; Rudolph, M.; Friedrich, M.; Görls, H.; Henry, W.; Vos, J. G. *Angew. Chem., Int. Ed.* **2006**, *45*, 6215–6218.

(8) (a) Fukushima, T.; Wada, T.; Ohtsu, H.; Tanaka, K. *Dalton Trans.* **2010**, *39*, 11526–11534. (b) Tannai, H.; Koizumi, T.-a.; Wada, T.; Tanaka, K. *Angew. Chem., Int. Ed.* **2007**, *46*, 7112–7115. (c) Koizumi, T.-a.; Tanaka, K. *Angew. Chem., Int. Ed.* **2005**, *44*, 5891–5894. (d) Polyansky, D.; Cabelli, D.; Muckerman, J. T.; Fujita, E.; Koizumi, T.-a.; Fukushima, T.; Wada, T.; Tanaka, K. *Angew. Chem., Int. Ed.* **2007**, *46*, 4169–4172. (e) Fukushima, T.; Fujita, E.; Muckerman, J. T.; Polyansky, D. E.; Wada, T.; Tanaka, K. *Inorg. Chem.* **2009**, *48*, 11510–1151. (f) Polyansky, D. E.; Cabelli, D.; Muckerman, J. T.; Fukushima, T.; Tanaka, K.; Fujita, E. *Inorg. Chem.* **2008**, *47*, 3958–3968.

(9) Padhi, S. K.; Kobayashi, K.; Masuno, S.; Tanaka, K. *Inorg. Chem.* **2011**, *50*, 5321–5323.

(10) Bomben, P. G.; Robson, K. C. D.; Sedach, P. A.; Berlinguette, C. P. *Inorg. Chem.* **2009**, *48*, 9631–9643.

(11) (a) Caspar, J. V.; Meyer, T. J. *Inorg. Chem.* **1983**, *22*, 2444. (b) Whitten, G. D. *Acc. Chem. Res.* **1980**, *13*, 83–90. (c) Matsubara, Y.; Koga, K.; Kobayashi, A.; Konno, H.; Sakamoto, K.; Morimoto, T.; Ishitani, O. *J. Am. Chem. Soc.* **2010**, *132*, 10547–10552. (d) Gholamkhass, B.; Mametsuka, H.; Koike, K.; Tanabe, T.; Furue, M.; Ishitani, O. *Inorg. Chem.* **2005**, *44*, 2326–2336.

(12) (a) *teXane version 1.11, Crystal Structure Analysis Package*; Molecular Structure Corporation/Rigaku Corporation: The Woodlands, TX, 2000. (b) Sheldrick, G. M. *SHELXS-97 and SHELXL-97*; University of Göttingen: Göttingen, Germany, 1997.

(13) (a) Meth-Cohn, O.; Narine, B.; Tarnowski, B. *Tetrahedron Lett.* **1979**, *20*, 3111–3114. (b) Patin, A.; Belmont, P. *Synthesis* **2005**, *14*, 2400–2406. (c) Chandra, A.; Singh, B.; Upadhyay, S.; Singh, R. M. *Tetrahedron* **2008**, *64*, 11680–11685.